Elucidating the 4f Binding Energy of an Isolated Pt Atom and Its Bulk Shift from the Measured Surface- and Size-Induced Pt 4f Core Level Shift

Yi Sun,[†] Yan Wang,[‡] Ji Sheng Pan,[†] Ling-ling Wang,[‡] and Chang Q. Sun*[,§,||]

*Institute of Materials Research and Engineering, A*STAR (Agency for Science, Technology and Research), 3 Research Link, Singapore 117602, School of Physics and Microelectronics Science, Hunan University, Changsha 410082, China, School of Electrical and Electronic Engineering, Nanyang Technological University, Singapore 639798, and Faculty of Materials, Optoelectronics and Physics and the Key Laboratory of Low-Dimensional Materials and Application Technologies (Ministry of Education), Xiangtan University, Hunan 411105, China*

Received: May 13, 2009; Revised Manuscript Received: June 13, 2009

Development of an approach extracting quantitative information regarding the energetic behavior of core electrons from photoelectron measurements of the surface and size dependence of core level variation has long been a challenge though the surface- and size-induced core level shifts of materials have been intensively investigated. Here we show that a combination of the tight binding theory, the bond order-length-strength (BOLS) correlation, and the measured data from Pt(111) surface and Pt nanocrystals has led to an approach for this purpose. With the developed method, we have analyzed the $4f_{7/2}$ core-level shift of four sets of data gained from the Pt(111) surface and four sets of data from Pt nanoclusters deposited on graphite and carbon nanotubes. Reconciliation of the measurements turns out that the Pt $4f_{7/2}$ binding energy of an isolated Pt atom and its bulk shift to be 67.67 and 2.99 eV, respectively. Consistency between the BOLS calculations and photoelectron measurements clarifies that the size- and surface-induced positive energy shifts originate from the broken-bond-induced local strain and the associated quantum trapping in surface of skin-depth while the bond length and binding energy in the core interior remain their bulk values. Reconciliation of the photoelectron measurements of both Pt(111) surfaces and Pt nanostructures evidence the reliability of the developed approach.

Downloaded by NANYANG TECH UNIV LIB on August 13, 2009
Published on July 6, 2009 on http://pubs.acs.org | doi: 10.1021/jp904445a

I. Introduction

Interaction between the under-coordinated atoms at sites surrounding atomic defects, terrace edges, or at surfaces of skin depth has been recognized as the key to the unusual behavior of low-dimensional systems such as atomic chains, nanoribbons, nanotubes, nanowires, nanograins, nanocavities, and the surface skin of a bulk specimen. The low-dimensional systems are characterized by a high fraction of atoms with an effective atomic coordination number (z or CN) being between 0 and 12.[1] z equals zero corresponds to an isolated atom and $z = 12$ to an atom in the ideal bulk interior (with an fcc structure as the standard). The elucidation of the electronic structure and the electronic binding energy of such low-dimensional systems is of great importance, since its clarification can improve our understanding of the origination of the novel physical properties of surfaces and nanostructures, such as the mechanical strength, chemical reactivity, thermal stability, optoelectronic, magnetic, and dielectric performance, as compared to those of the bulk counterparts.[2] From the spectra of X-ray photoelectron spectroscopy (XPS), the binding energies (BE), being a superposition of the intra-atomic trapping and the interatomic binding (crystal potential) contributions, of various elements can be determined through discrimination of these two components. An increase in core-level BE with decreasing particle size has been observed frequently in numerous species such as Au, Ag, Ni, Cu, Pd, Si, C, etc., and their compounds as well.[3−9] For instances, calculations[10] suggested that the 2p binding energies of Cu_{18} and Ni_{18} atomic clusters undergo positive shifts from their bulk values (taking as zero) to 0.7−0.8 eV when the average strain of the clusters are increased from zero to 6%. A combination of scanning tunneling microscopy/spectroscopy measurements and density functional theory as well as molecular dynamics calculations revealed that the mean lattice constant of Co nanoislands contracts by 6% from the bulk value of 0.251 to 0.236 nm from the center to the edge of the nanoislands deposited on copper substrates;[11] an apparent energy shift of ∼0.2 eV of the occupied valence states has been detected when the island size is reduced from 22.5 to 4.8 nm.[12] Measurements using X-ray absorption spectroscopy, Reif et al.[13] have discovered that the Cr-2p level shifts monotonically from the 2p BE of an isolated Cr atom at 573.5 eV, by ∼0.9 eV, to the 2p BE of a 13-atom cluster at 574.4 eV.

The surface- and size-induced Pt BE shift is of particular interest as the Pt surfaces and nanostructures are promising candidates for catalytic oxidation of carbon monoxide and nitric monoxide species.[14−18] Using XPS, Marcus et al.[19] and Yang et al.[20] have measured an ∼0.6 eV increase of the Pt $4f_{7/2}$ BE from 71.1 eV for the bulk Pt surface to 71.7 eV for Pt nanoclusters deposited on carbon nanotubes; Yang et al.[21] found an ∼0.5 eV increase from the bulk value to 71.6 eV for ∼0.4 monolayers (ML) Pt deposited on HOPG; Bittencourt et al.[22] also reported an increase of ∼0.5 eV in the BE of Pt $4f_{7/2}$ from 71.4 eV for 2 nm to 72.0 eV for 0.2 nm, equivalent to 0.9 ML, of Pt deposited on the CNT. Bianchettin et al.[23] examined the

* To whom correspondence should be addressed. E-mail: ecqsun@ntu.edu.sg.
[†] A*STAR.
[‡] Hunan University.
[§] Nanyang Technological University.
[||] Xiangtan University.

10.1021/jp904445a CCC: $40.75 © 2009 American Chemical Society
Published on Web 07/06/2009

Downloaded by NANYANG TECH UNIV LIB on August 13, 2009
Published on July 6, 2009 on http://pubs.acs.org | doi: 10.1021/jp904445a

coordination effect on the $4f_{7/2}$ BE shift of Pt(111) surface upon deposition of Pt_n ($n = 1-10$) adatoms and found the adatoms could increase the intensity of the high-energy component of the decomposed spectra. These observations showed clearly that both surface and particle size could induce positive BE shifts of Pt nanostructures because of the reduction of effective atomic CNs.

Although various models have been developed, quantifying the extent of crystal binding energy in a bulk specimen in contrast to the intra-atomic trapping energy experienced by the 4f electrons of an isolated Pt atom and understanding the origin of the surface- and size-induced core-level BE shift still remain challenging.[5] It needs to be clarified that we should consider the BE shift from the bulk value or from that of an isolated atom. The "initial (neutral)−final (ionized) state" effect was elegantly accepted to explain the BE shifts as arising from the poor screening of the core−hole, but experimental and theoretical results have shown that this model could not account for all of the observations.[24,25] Subsequently, another mechanism suggested that with increasing particle size, the metal nanoparticle undergoes a transition from metallic to a structure with nonmetallic properties, which was also found to be insufficient after comparison with experimental results.[26] Therefore, it is highly desirable to gain deeper insight into the mechanism of the BE shift and to derive quantitative information regarding the BE of an isolated atom and its bulk shift from the measurements. In this work, we analyzed four sets of XPS $4f_{7/2}$ spectra from Pt(111) surface and four sets of data from Pt nanoclusters deposited on carbon to extract information regarding the energy level of an isolated Pt atom and its bulk shift by matching theory with measurements. Meanwhile, we clarify that the surface- and size-induced BE shift arises from the broken-bond-induced local strain and skin-depth quantum trapping.

II. Principle

2.1. BOLS Initiated Hamiltonian Perturbation. The recently developed bond order-length-strength (BOLS) correlation mechanism[2] states that the remaining bonds of an under-coordinated atom, which occurs due to the breakage of one or more of its initial bonds, contract and strengthen spontaneously, contributing to an increase in the bond energy. This leads to the formation of a local strain and quantum trapping, and also the densification of charge and energy at local sites around the original atomic defect, which occurs frequently at the surface or skin depth of nanostructures. The development of this strain-induced quantum trapping forms a perturbation to the Hamiltonian of the originally extended structure due to the unusual boundary conditions. With this physical picture of atomic CN imperfection as the basis, the BOLS can account for the size-induced core level shifts, band gap expansion, solid−liquid transition, and surface and nanostructure mechanical strength.[2] Furthermore, the ability of the BOLS to calculate the energy levels of an isolated atom and the energy shift of the bulk sample with great sensitivity, i.e., to make the distinction between the effects of the interatomic binding versus the intra-atomic trapping potential on the electron, has not yet been achieved by other theoretical approaches. This can be done via two routes: either based on XPS measurements of the BE's of samples of varying dimensions (size effect) or from the decomposition of a single BE peak spectrum from a well-defined surface (surface effect).

Quantitatively, the BOLS correlation provides the following relationships between the atomic CN, bond length and bond energy

$$\begin{cases} c_i = d_i/d = 2/[1 + \exp((12 - z_i)/8z_i)] \\ E_i = c_i^{-m} E_b \end{cases} \quad (1)$$

The contracted length of a bond of an under-coordinated surface atom in the ith layer, d_i, is related to the length of a bond in the bulk solid of the same material, d, by the bond contraction coefficient, c_i. This parameter is dependent on the coordination of the atom, z_i. The z_1 ($i = 1$) is curvature dependent, which follows a $4 \times (1-0.75K^{-1})$ relation, where $K = R/d$ is the number of atoms lined along the radius of the spherical solid and K^{-1} is also the curvature of the specimen. For a flat surface, $K^{-1} = 0$; for a spherical solid, $K^{-1} > 0$; for a hollow cave, $K^{-1} < 0$. $z_2 = z_1 + 2$ and $z_3 = 12$ are sufficient to describe all the nanostructures with various curvatures. Also, the magnitude of a remaining bond's BE of an under-coordinated surface atom (E_i) increases as the bonds contract spontaneously, and is equal to the "c_i^{-m}" multiple of the energy of a single bond in a bulk sample (E_b). The parameter m, which is not freely adjustable, characterizes the nature of a bond in a solid, or otherwise deciphered as the parameter relating the bond energy to its length. From available experimental data, m was determined to be approximately four for compounds and alloys and approximately one for metals.

From the energy band theory and the BOLS correlation, the Hamiltonian of the crystal undergoes the perturbation Δ_H due to the atomic CN deficiency experienced by surface atoms and those in adjacent layers to the crystal potential, $V_{crys}(r)$, while the intra-atomic trapping, $V_{atom}(r)$, remains unchangeable[27]

$$V(\Delta_i) = V_{atom}(r) + V_{crys}(r)[1 + \Delta_H]$$

where

$$\begin{cases} \Delta_H = \sum_{i\le 3} \gamma_i \Delta_i = \tau K^{-1} \sum_{i\le 3} c_i \Delta_i = \Delta_H' \tau K^{-1} (\text{Nanotructure}) \\ \Delta_i = c_i^{-m} - 1 (\text{Surface}) \end{cases} \quad (2)$$

Here, $\sum_{i \le 3} c_i \Delta_i = \Delta_H'$ and $\gamma_i = \tau c_i K^{-1}$ is the surface-to-volume ratio, proportional to τ ($\tau = 1$, 2, and 3 corresponds to the dimensionality of a thin plate, a cylindrical rod, and a spherical dot, respectively), and inversely proportional to the dimensionless size K. The Δ_H sums over only the outermost three atomic layers; the Δ_i represents the perturbation to the individual ith surface layer. For $i > 3$, the atomic bonds are assumed to be set sufficiently deep into the bulk of the solid such that they do not experience significant deficiencies in atomic CN, unlike those at and near the surface. Recent electron diffraction experiment[28] revealed that only the atoms in the outermost two atomic layers of gold nanoclusters experience contractions. Scanning tunneling microscopy measurement under tension at 4K revealed that the maximal Pt−Pt bond length in a monatomic chain, with an effective $z = 2$, before breaking is 0.23 ± 0.02 nm, being $83 \pm 7\%$ of the bulk value of 0.277 nm.[29] The equilibrium (without tension) Pt−Pt bond length is expected to be 70% of the bulk value according to the current BOLS mechanism. Most strikingly, a recent X-ray absorption diffraction spectroscopic study[30] revealed that the Ni 2p levels of the outermost three atomic layers shift positively to higher binding energy discretely, with the outermost atomic layer shifting the most. From the electronic structure point of view, the surface consists of at most three atomic layers or two interatomic

spacings. Therefore, only the under-coordinated atoms in the surface skin contribute to the additional perturbation Δ_H to the overall Hamiltonian. The Δ_H (τ, K, K^{-1}; m, z_i, d_i, E_i) covers all the possible extrinsic contributions from the shape, size, curvature and the intrinsic contributions from bond nature, order, length and energy to the Hamiltonian. Chemical reaction or externally thermal and mechanical stimulations will modulate the m, d_i, and E_i values and hence the Hamiltonian.

2.2. $E_\nu(1)$ and $\Delta E_\nu(\infty)$ Determination. Incorporating the BOLS correlation into the band theory with the size-induced Hamiltonian perturbation, the energy shift of a specific νth energy level of a nanostructure or a surface layer with respect to that of an isolated atom is

$$\Delta E_\nu(K) = E_\nu(K) - E_\nu(1) = \Delta E_\nu(\infty)(1 + \Delta_H) = [E_\nu(\infty) - E_\nu(1)](1 + \Delta_H)$$

where

$$\begin{cases} E_\nu(1) & = \langle \phi_\nu(r)|V_{atom}(r)|\phi_\nu(r)\rangle & \text{(Core level energy)} \\ \Delta E_\nu(\infty) & = \beta + z\gamma \propto \langle E_0\rangle & \text{(Core level shift)} \\ \beta & = \langle \phi_\nu(r)|V_{cry}(r)|\phi_\nu(r)\rangle \propto \langle E_b\rangle & \text{(Exchange integral)} \\ \gamma & = \langle \phi_\nu(r)|V_{cry}(r)|\phi_\nu(r')\rangle \propto \langle E_b\rangle & \text{(Overlap integral)} \end{cases} \quad (3)$$

The intra-atomic trapping potential, $V_{atom}(r)$, determines the νth energy level of an isolated atom, $E_\nu(1)$. The $\phi_\nu(r)$ ($r \neq r'$) is the specific Bloch wave function at site r. The parameter z is the weighting factor of the overlapping integral contribution to the $\Delta E_\nu(\infty)$. For a monatomic chain, $z = 2$. Because of the strong localization nature of the core electrons, the overlapping integral is negligibly small compared with the exchange integral. Therefore, the interatomic bond energy, $\langle E_b\rangle$, dominates the shift of binding energy. Equation 3 can be reorganized as

$$\frac{E_\nu(K) - E_\nu(1)}{E_\nu(\infty) - E_\nu(1)} = 1 + \begin{cases} \Delta_H = \Delta\tau K^{-1} & \text{(Nanostructure)} \\ \Delta_i = c_i^{-1} - 1 & \text{(Surface component)} \end{cases}$$

or

$$\frac{E_\nu(K) - E_\nu(\infty)}{E_\nu(\infty) - E_\nu(1)} = \begin{cases} \Delta_H = \tau\Delta K^{-1} & \text{(Nanostructure)} \\ \Delta_i & \text{(Surface component)} \end{cases} \quad (4)$$

For the surface BE shift, we have the relation

$$\frac{E_\nu(i) - E_\nu(1)}{E_\nu(i) - E_\nu(1)} = \frac{c_i}{c_i}, \quad (i = S_1, S_2, B; i \neq i)$$

which yields

$$\begin{cases} E_\nu(1) & = \dfrac{c_i^{-1}E_\nu(i) - c_i^{-1}E_\nu(i)}{c_i^{-1} - c_i^{-1}} \\ \Delta E_\nu(\infty) & = [E_\nu(i) - E_\nu(1)]c_i \end{cases} \quad (5)$$

Therefore, a proper decomposition of the surface BE spectrum will allow us to estimate the $E_\nu(1)$ and $\Delta E_\nu(\infty)$, with the given c_i values that have been extensively verified.[1,2]

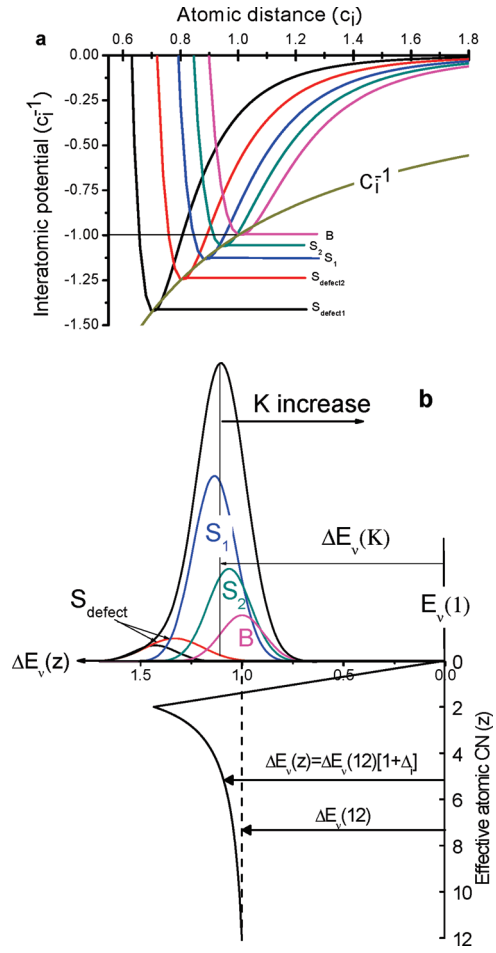

Figure 1. (a) Illustration of the BOLS correlation and (b) atomic CN resolved core level shift. Bond order deficiency induced bond contraction (c_i) and the associated interatomic potential depression (c_i^{-1}). The broken-bond-induced local strain and the quantum trapping perturb the Hamiltonian that determines the BE shift from the BE of an isolated atom, $E_\nu(z = 0)$. $S_1(z = 4)$ and S_2 ($z = 6$) represent the first and the second surface layers and B ($z = 12$) the bulk contribution. S_{defect} ($z = 2, 3$) represents the contribution from adatoms or edges atoms. Please refer to ref 40 for a surface structure model for the effective CN of the S_i. The energy of the convoluted envelope changes with solid size because of the variation of surface-to-volume ratio. The energy shift of each component satisfies the relation: $\Delta E_\nu(i):\Delta E_\nu(B) = E_i:E_b = c_i^{-m}(i = S_{defect}, S_1, S_2)$.

TABLE 1: Information Derived from the Original Decomposition of the Pt(111) Spectrum with Only Two Components B and S_1[a]

refs	B	S_1	S_1-B	$\Delta E_{4f}(\infty)$	$E_{4f}(1)$
17	70.78	71.21	0.43	3.07	67.71
18	70.59	71.01	0.42	2.99	67.59
23	70.73	71.14	0.41	2.87	67.86
31	70.53	70.96	0.43	3.03	67.50
average	70.66	71.08	0.42	2.99	67.67

[a] S_1-B is the energy separation from which we can derive the value of $\Delta E_{4f}(\infty)$ with $E_{4f}(1)$ as the referencing point of energy shift. It is clear that the conventionally referred bulk value corresponds to the S_1 peak energy.

Generally, the size-induced BE shifts of nanostructures exhibit an inversely linear relationship with the nanosolid size K, in the form of $E_\nu(K) = A + CK^{-1}$, where A and C are constants that can be determined by finding the y-intercept and gradient, respectively, of a linear fit to a set of measured BE energy versus solid size. Comparing the experimental

Downloaded by NANYANG TECH UNIV LIB on August 13, 2009
Published on July 6, 2009 on http://pubs.acs.org | doi: 10.1021/jp904445a

scaling relationship with the theoretical expression derived from eq 4 yields

$$E_\nu(K) = \begin{cases} E_\nu(\infty) + [E_\nu(\infty) - E_\nu(1)]\tau\Delta K^{-1} & \text{(BOLS theory)} \\ A + CK^{-1} & \text{(Measurement)} \end{cases}$$

Equating the theory prediction to measurement gives A as the energy of a bulk sample, $E_\nu(\infty)$, and C's relation to the νth energy level shift from that of an isolated atom to the bulk, $\mathbf{\Delta}E_\nu(\infty)$, the dimensionality τ and the surface Hamiltonian perturbation Δ'_H:

$$\begin{cases} C = [E_\nu(\infty) - E_\nu(1)]\tau\Delta \\ A = E_\nu(\infty) \end{cases} \quad (6)$$

From eq 6, the νth energy level of an isolated atom and its bulk shift can be calculated using the relations

$$\begin{cases} E_\nu(1) = A - \dfrac{C}{\tau\Delta_H} & \text{(Atomic energy level)} \\ \Delta E_\nu(\infty) = \dfrac{C}{\tau\Delta_H} & \text{(Bulk shift)} \end{cases} \quad (7)$$

Using eqs 5 and 7, we can readily determine the energy level $E_\nu(1)$ of an isolated atom and its bulk shift $\Delta E_\nu(\infty)$ through analyzing the measurements. Combining eqs 5 and 7, we have the form for the surface and size-induced core level shift

$$E_\nu(K) = E_\nu(1) + \Delta E_\nu(\infty) \times \begin{cases} (1 + \Delta'\tau K^{-1}) & \text{(nanostructure)} \\ [c(z)]^{-1} & \text{(surface component)} \end{cases} \quad (8)$$

Figure 1, panel a, illustrates the BOLS correlation and panel b the associated BE shift of each component. Broken-bond-induced local strain and quantum trapping modifies the equilibrium bond length and bond energy; the BE shift is proportional to the bond energy at equilibrium. $S_1(z = 4)$ and S_2 ($z = 6$) correspond to the outermost and the second atomic layer and B the bulk components. S_{defect} ($z = 2$ or 3) represents the adatoms or atoms at edges with even lower atomic CNs. The convolution of these components will change with solid size because of the varied contributions from each component. For a surface, the peak energies of the components may fluctuate slightly with varying experimental conditions such as temperature, crystal orientation, and incident radiation beam angle.[5]

Figure 1b also shows the BOLS expected trend of atomic-CN resolved BE shift from the $E_\nu(1)$. The initial part from $z = 0$ to a value around 1 or 2 is in good agreement with observations from Cr atomic clusters.[13] The skin-depth potential trapping causes the energy pinning and densification and hence the core-level shift for each component that is proportional to the magnitude of bond energy in the relation: $\Delta E_\nu(i):\Delta E_\nu(B) = E_i:E_b = C_i^{-m}(i = S_{defect}, S_1, S_2)$. The energy dependence of the envelope shift follows eq 8.

III. Results and Discussion

3.1. Pt Surface 4f BE Shift. According to available database, the XPS $4f_{7/2}$ spectra from Pt(111) clean surface[17,18,23,31] can be decomposed into two components S_1 and B with the peak values listed in Table 1. Taking the mean peak values of S_1 and B, we can find the separation $E(S_1) - E(B)$ and calculate the bulk shift using eq 5, which gives the value of $E(\infty) - E(1) = [E(S_1) - E(B)]/[c_z^{-1}{}_{=4} - 1] = 2.99$ eV. According to the BOLS expectation, the XPS spectrum can be decomposed into at least three components representing S_1, S_2, and B; the defect component S_{defect} provides an addition that should be above the S_1 because of the even lower atomic CNs of adatoms or defects. The initially assigned S and B component order corresponding to negative shift is not in line with the consequence of tight binding or the BOLS theory. The peak positions of the components satisfy the relation: $\Delta E_\nu(i):\Delta E_\nu(B) = E_i:E_b = c_i^{-1}(i = S_{defect}, S_1, S_2)$. The peak intensity of each component is subject to surface experimental conditions. Figure 2 shows a typically decomposed Pt(111)-$4f_{7/2}$ spectrum with the expected components with respect to the BOLS expected trend of atomic-CN resolved BE shift from the $E_{4f}(1)$ of a specimen.

3.2. Pt Nanostructure Core Level Shift. A linear fitting to the measured data[19−22] has been conducted to obtain A and C from the plot of BE peak energy (the energy at which the maximum intensity of the Pt $4f_{7/2}$ signal occurs) of Pt $4f_{7/2}$ vs the inverse of layer thickness (1/K, in units of 1/monolayer (ML), where 1 ML of Pt is approximated to 0.278 nm, the diameter of a Pt atom). The errors of A and C are the standard deviations obtained from the linear fittings, while the errors of $E_\nu(\infty)$ and $E_\nu(1)$ are propagated via the quadrature of the sum of the previous errors.

As in the BOLS convention, $z_{1,2,3}$ were taken to be 4, 6, and 12, respectively, with $m = 1$ for metals. From the relation of $c_i(z_i)$ in eq 1, $c_{1,2,3}$ were calculated to be 0.8757, 0.9376, and 1, respectively, from which $\Delta'_{1,2,3} = 0.1243$, 0.0624, and 0, respectively, giving $\Delta'_H = \Delta'_1 + \Delta'_2 = 0.1868$, which is used in the determination of $\Delta E_{4f}(\infty)$ and $E_{4f}(1)$. The derived values are given in Table 2. If we use the apparent CN $z_{1,2,3} = 8$, 10, and 12, $c_{1,2}$ will be 0.9688 and 0.9875, $\Delta'_H = \Delta'_1 + \Delta'_2 =$

TABLE 2: Estimation of Energy Levels of an Isolated Pt Atom, $E_\nu(1)$, and of Bulk Atom, $E_\nu(\infty)$, or Pt Nanoparticles Evaporated onto CNT or HOPG Surfaces[a]

Pt deposited on carbon	$A = E_{4f}(\infty)$	C	$E_{4f}(1)$	$\Delta E_{4f}(\infty)$ ($\tau = 1.05$)
HOPG[19]	71.16 ± 0.03	0.67 ± 0.13		
HOPG[21]	71.12 ± 0.03	0.60 ± 0.08		
CNT[20]	71.16 ± 0.03	0.48 ± 0.08		
CNT[22]	71.29 ± 0.10	0.61 ± 0.28		
mean value of $4f_{7/2}$	71.18 ± 0.10	0.59 ± 0.28	68.19 ± 0.30	2.99 ± 0.31
offset to match surface	71.08(S_1)	70.66(B)	67.67	
Pt $4f_{7/2}$ bulk reference	71.10[19]			

[a] The experimental data of binding energy peak vs $1/K$ (1 ML of Pt is taken as the Pt atomic diameter = 0.278 nm) is fit with a linear relation to obtain the intercept, A, and the slope, C, from which $E_\nu(1)$, $E_\nu(\infty)$, and hence the energy shift $\Delta E_\nu(\infty)$ can all be estimated. It is clear that the conventionally referred bulk value of 71.10 eV corresponds to the S_1 peak energy, 71.08. Using the apparent CN of 8 and 10 for the outermost two atomic layers will lead to the $\Delta E_{4f}(\infty) \sim 12.78$ eV that is unreasonably higher than even the atomic cohesive energy of 5.84 eV per Pt atom.[1,2]

Downloaded by NANYANG TECH UNIV LIB on August 13, 2009
Published on July 6, 2009 on http://pubs.acs.org | doi: 10.1021/jp904445a

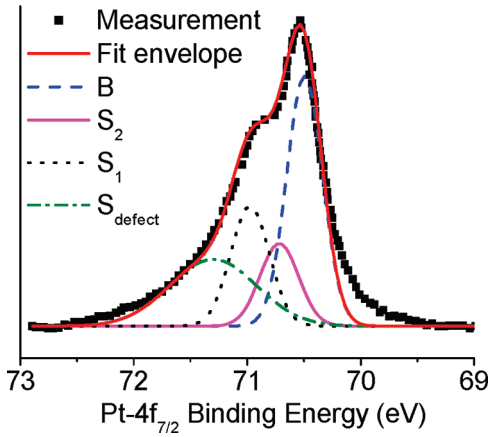

Figure 2. Typical decomposition of the Pt $4f_{7/2}$ spectrum from Pt(111) surface[19] with four components of S_1, S_2, B, and S_{defect}. The decomposition is subject to the conditions: (i) the total number of peaks is at least three; (ii) the peak position of the components satisfy the relation: $\Delta E_{4f}(i):\Delta E_{4f}(B) = E_i:E_b = c_i^{-1}(i = S_{defect}, S_1, S_2)$; (iii) the peak width of the components should be constrained with a certain range; (v) the intensity of each component is subject to surface condition and experimental conditions. The deviation from the prediction at the lower end of size may involve contribution from the negative curvature effect, or hollow structures, surrounding the C−C bond in the CNTs. The negative curvature leased to the higher coordination and hence weaker binding energy.

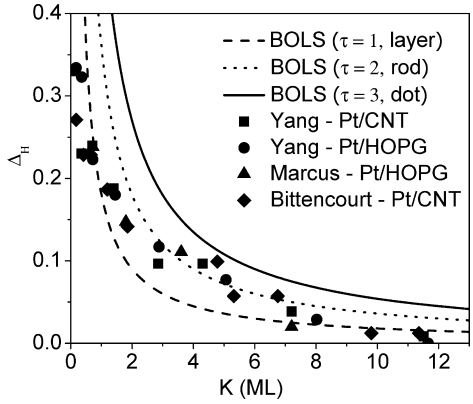

Figure 3. Numerically matching the relative energy shifts, $\Delta_H = [E_{4f}(K) - E_{4f}(\infty)]/[E_{4f}(\infty) - E_{4f}(1)]$, for Pt $4f_{7/2}$ deposited on MWCNT and HOPG surfaces, as computed from their respective $E_{4f}(\infty)$ and $E_{4f}(1)$ presented in Table 2.

0.0437. The $E_{4f}(\infty) - E_{4f}(1) = 2.99$ eV $\times$ 0.1868/0.0437 = 12.78 eV is unreasonably higher than the atomic cohesive energy of 5.84 eV per Pt atom. From the TEM images of Pt nanoparticle growth,[20,21] it was found that the Pt forms in patches without certain of the τ value. With the value of $E_{4f}(\infty) - E_{4f}(1) = 2.99$ eV derived from surface analysis, we can then determine the shape factor $\tau = 1.0535$ in the size dependent spectra. τ approaching unity means that the observed patches proceed in a layer-by-layer pattern of growth. At the lower end of size, there is a deviation from the prediction, which may include contribution from the negative curvature effect, or hollow structures, of clusters surrounding the C−C bond in the CNTs. The negative curvature leased to the higher coordination and hence weaker binding energy. The accuracy of the derivatives is subject to the precision in measurement and the particle size determination. The equivalent monolayer size reference in the measurement may need examination. According to the TEM observations, the dimensionality of the Pt patches should be greater than unity. Using the equivalent thickness may therefore render a possible underestimation of the τ value for the nanoclusters.

The relative energy shifts, $\Delta_H = [E_{4f}(K) - E_{4f}(\infty)]/[E_{4f}(\infty) - E_{4f}(1)]$, are plotted against K (ML) for Pt $4f_{7/2}$, as shown in Figure 3. Comparing the XPS reference data for bulk Pt $4f_{7/2}$ BE, 71.1 eV,[19] it is clarified that the previously referred bulk BE energy around 71.1 eV corresponds to the S_1 component for the flat surface. The bulk component should be 70.66 eV, instead.

Combining the surface- and size-induced core level shift, we have the general form for the core level shift

$$E_{4f}(i) = E_{4f}(1) + \Delta E_{4f}(\infty)\begin{cases} c_i^{-1} \\ (1 + \Delta'_H \times \tau K^{-1}) \end{cases}$$
$$= 67.67 + 2.99 \times \begin{cases} c_i^{-1} & \text{(Pt surface)} \\ (1 + 0.1968K^{-1}) & \text{(Pt/C)} \end{cases} \quad (9)$$

One may be concerned about the PtC interface contribution to the measurement because of the possible bond contraction and band nature alteration.[1] However, XPS measurements[4] revealed that the C-1s binding energy does not shift when the Au coverage on the CNT is increased.[4] Furthermore, C−Pt bond can hardly form at temperature below 630 K.[32] Argon or oxygen plasma bombardment of carbon surfaces only introduce defects[33−36] that will introduce additional defect states S_{defect} as illustrated in Figure 1b. Therefore, interface contribution to the core level shift can be neglected in the analysis.

Consistency between theory calculations and measurements suggests that the observed energy shifts result from the size-induced lattice strain and the associated skin-depth quantum trapping for small clusters or surface interlayer relaxation of a bulk solid, which agrees with the previously recommended mechanism of surface interlayer strain and charge densification.[37−39]

IV. Conclusion

A combination of the new degree of freedom of solid size, the XPS technique, the band theory and the BOLS correlation has enabled us to extract information about the Pt 4f binding energy of an isolated atom and its shift upon bulk formation from matching four sets of XPS data collected from Pt(111) surface and Pt nanoclusters. It has been clarified that the BE shift arises from intrinsically the skin-depth strain and quantum trapping. Understanding may be extended to the enhancement of catalytic effect of nanostructured Pt as the BE shift also happens to the valence band, which will enhance the electroaffinity of the small samples.

Acknowledgment. Financial supports by the Agency for Science, Technology and Research (A*STAR) and Nanyang Technological University, National Natural Science Foundation of China (No.10772157), Hunan Province, and the Key Laboratory of New Ceramics and Refinery Processing at Tsinghua University, China are gratefully acknowledged.

References and Notes

(1) Sun, C. Q. *Prog. Mater. Sci.* **2009**, *54*, 179.
(2) Sun, C. Q. *Prog. Solid State Chem.* **2007**, *35*, 1.
(3) Balamurugan, B.; Maruyama, T. *J. Appl. Phys.* **2007**, *102*, 034306.
(4) Bittencourt, C.; Felten, A.; Douhard, B.; Ghijsen, J.; Johnson, R. L.; Drube, W.; Pireaux, J. J. *Chem. Phys.* **2006**, *328*, 385.
(5) Sun, C. Q. *Phys. Rev. B* **2004**, *69*.

Downloaded by NANYANG TECH UNIV LIB on August 13, 2009
Published on July 6, 2009 on http://pubs.acs.org | doi: 10.1021/jp904445a

(6) Suprun, S. P.; Fedosenko, E. V. *Semiconductors* **2007**, *41*, 590.
(7) Aruna, I.; Mehta, B. R.; Malhotra, L. K.; Shivaprasad, S. M. *J. Appl. Phys.* **2008**, *104*.
(8) Tao, J. G.; Pan, J. S.; Huan, C. H. A.; Zhang, Z.; Sun, Y.; Chai, J. W.; Wang, S. J. *J. Phys.: Condens. Matter* **2008**, *20*.
(9) Tao, J. G.; Pan, J. S.; Huan, C. H. A.; Zhang, Z.; Chai, J. W.; Wang, S. J. *Surf. Sci.* **2008**, *602*, 2769.
(10) Richter, B.; Kuhlenbeck, H.; Freund, H. J.; Bagus, P. S. *Phys. Rev. Lett.* **2004**, *93*.
(11) Mironets, O.; Meyerheim, H. L.; Tusche, C.; Stepanyuk, V. S.; Soyka, E.; Hong, H.; Zschack, P.; Jeutter, N.; Felici, R.; Kirschner, J. *Phys. Rev. B* **2009**, *79*, 035406.
(12) Mironets, O.; Meyerheim, H. L.; Tusche, C.; Stepanyuk, V. S.; Soyka, E.; Zschack, P.; Hong, H.; Jeutter, N.; Felici, R.; Kirschner, J. *Phys. Rev. Lett.* **2008**, *100*, 096103.
(13) Reif, M.; Glaser, L.; Martins, M.; Wurth, W. *Phys. Rev. B* **2005**, *72*, 155405.
(14) Fauth, K.; Schneider, N.; Hessler, M.; Schutz, G. *Eur. Phys. J. D* **2004**, *29*, 57.
(15) Hu, Z. Y.; Boiadjiev, V.; Thundat, T. *Energy Fuels* **2005**, *19*, 855.
(16) Gunther, S.; Scheibe, A.; Bluhm, H.; Haevecker, M.; Kleimenov, E.; Knop-Gericke, A.; Schlogl, R.; Imbihl, R. *J. Phys. Chem. C* **2008**, *112*, 15382.
(17) Lin, T. H.; Huang, T. P.; Liu, Y. L.; Yeh, C. C.; Lai, Y. H.; Hung, W. H. *Surf. Sci.* **2005**, *578*, 27.
(18) Zhu, J. F.; Kinne, M.; Fuhrmann, T.; Denecke, R.; Steinruck, H. P. *Surf. Sci.* **2003**, *529*, 384.
(19) Marcus, P.; Hinnen, C. *Surf. Sci.* **1997**, *392*, 134.
(20) Yang, D. Q.; Sacher, E. *J. Phys. Chem. C* **2008**, *112*, 4075.
(21) Yang, D. Q.; Sacher, E. *Chem. Mater.* **2006**, *18*, 1811.
(22) Bittencourt, C.; Hecq, M.; Felten, A.; Pireaux, J. J.; Ghijsen, J.; Felicissimo, M. P.; Rudolf, P.; Drube, W.; Ke, X.; Van Tendeloo, G. *Chem. Phys. Lett.* **2008**, *462*, 260.
(23) Bianchettin, L.; Baraldi, A.; de Gironcoli, S.; Vesselli, E.; Lizzit, S.; Petaccia, L.; Comelli, G.; Rosei, R. *J. Chem. Phys.* **2008**, *128*, 114706.
(24) Vijayakrishnan, V.; Chainani, A.; Sarma, D. D.; Rao, C. N. R. *J. Phys. Chem.* **1992**, *96*, 8679.
(25) Pehlke, E.; Scheffler, M. *Phys. Rev. Lett.* **1993**, *71*, 2338.
(26) Rao, C. N. R.; Kulkarni, G. U.; Thomas, P. J.; Edwards, P. P. *Chem.—Eur. J.* **2002**, *8*, 29.
(27) Sun, C. Q.; Fu, S. Y.; Nie, Y. G. *J. Phys. Chem. C* **2008**, *112*, 18927.
(28) Huang, W. J.; Sun, R.; Tao, J.; Menard, L. D.; Nuzzo, R. G.; Zuo, J. M. *Nat. Mater.* **2008**, *7*, 308.
(29) Smit, R. H. M.; Untiedt, C.; Yanson, A. I.; van Ruitenbeek, J. M. *Phys. Rev. Lett.* **2001**, *87*, 266102.
(30) Matsui, F.; Matsushita, T.; Kato, Y.; Hashimoto, M.; Inaji, K.; Guo, F. Z.; Daimon, H. *Phys. Rev. Lett.* **2008**, *100*.
(31) Apai, G.; Baetzold, R. C.; Shustorovich, E.; Jaeger, R. *Surf. Sci.* **1982**, *116*, L191.
(32) Nakamura, J.; Hirano, H.; Xie, M. S.; Matsuo, I.; Yamada, T.; Tanaka, K. *Surf. Sci.* **1989**, *222*, L809.
(33) Yang, D. Q.; Sacher, E. *Surf. Sci.* **2002**, *516*, 43.
(34) Wang, Y. F.; Ye, Y. C.; Wu, K. *Surf. Sci.* **2006**, *600*, 729.
(35) Osvath, Z.; Vertesy, G.; Tapaszto, L.; Weber, F.; Horvath, Z. E.; Gyulai, J.; Biro, L. P. *Electron. Properties Novel Nanostruct.* **2005**, *786*, 154.
(36) Paredes, J. I.; Martinez-Alonso, A.; Tascon, J. M. D. *Langmuir* **2007**, *23*, 8932.
(37) Bartynski, R. A.; Heskett, D.; Garrison, K.; Watson, G.; Zehner, D. M.; Mei, W. N.; Tong, S. Y.; Pan, X. *J. Vac. Sci. Technol., A* **1989**, *7*, 1931.
(38) Fang, B. S.; Lo, W. S.; Chien, T. S.; Leung, T. C.; Lue, C. Y.; Chan, C. T.; Ho, K. M. *Phys. Rev. B* **1994**, *50*, 11093.
(39) Balasubramanian, T.; Andersen, J. N.; Wallden, L. *Phys. Rev. B* **2001**, *64*, 205420.
(40) Sun, Y.; Pan, J. S.; Tao, J. G.; Nie, Y. G.; Huan, C. H. A.; Zhang, Z.; Chai, J. W.; Li, D.; Wang, S. J.; Sun, C. Q. *J. Phys. Chem. C* **2009**, *113*, 10939.

JP904445A

Downloaded by NANYANG TECH UNIV LIB on August 13, 2009
Published on July 6, 2009 on http://pubs.acs.org | doi: 10.1021/jp904445a